Journal of Structural Geology, Vol. 13, No. 3, pp. 275 to 280, 1991
Printed in Great Britain

0191-8141/91 $03.00+0.00

The interpretation of fold axial data from regions of polyphase folding

KIERAN F. MULCHRONE

Department of Geology, University College, Cork, Eire

(*Received* 27 *April* 1989; *accepted in revised form* 28 *June* 1990)

Abstract—A region with two interfering fold phases is considered. If it is assumed that the early (F_n) and later (F_{n+1}) fold phase are cylindrical and that F_{n+1} formed by shear folding, then it is shown how the *a*- and *b*-directions of F_{n+1} can be determined. A technique for determining the original orientation of F_n and S_n is presented provided that similar amounts of simple shear occurred on opposing limbs of F_{n+1} folds. The cause of variability in fold axial orientations is investigated and information to be extracted from fold axial distributions is presented.

INTRODUCTION

INTERPRETATION of data from regions with polyphase folding conventionally involves recognition of fold axes and axial planes in the large scale, thus allowing subdivision of the study area. Hence, by plotting poles to the reference foliation (i.e. bedding), one obtains information regarding the present orientation of the dominant structures (Ragan 1985, Ramsay & Huber 1987). Such an analysis may not always be possible, particularly in strongly deformed regions, where fold phases may be isoclinal in nature. However, the recognition of structures in the small scale is usually feasible. The method developed below essentially deals with the interpretation of small-scale fold axial data which allows extraction of information from even highly deformed areas, provided the inherent assumptions are justifiable.

SHEAR FOLDING

To explain the development of similar folds, shear folding has been postulated (Ramsay 1967, pp. 430–436). During an episode of shear folding (F_n) two mutually perpendicular directions, a_n and b_n, define the shear plane, with a_n defining the absolute movement azimuth. The fold axis need not always parallel the b_n-direction. Two properties of shear folding are incorporated within this contribution:

(i) the fold axis produced when a plane of any orientation undergoes shear folding will always lie in the shear plane. This is always the case unless the given plane initially contained the a_n-direction;

(ii) any pre-folding linear fabric which was not an element of the shear plane will constitute a planar distribution after folding (Ramsay 1967, Ramsay & Huber 1987).

APPLICATION TO SHEAR FOLDING

Prior to applying the above properties to superposed folding, three assumptions must be entirely justified before the theory developed below can be satisfactorily applied:

(i) the earliest fold phase under consideration (F_n) acted on a pre-existing planar foliation (S_{n-1}), i.e. bedding or a planar tectonic fabric, that was uniform in orientation throughout the study area;

(ii) with or without a pure shear component the later fold phase (F_{n+1}) formed via shear folding;

(iii) both fold phases must be cylindrical in nature.

If a component of pure shear is associated with F_{n+1}, then the kinematic axes of the simple shear component of F_{n+1} will still be calculable. However, in such a case the original orientation of F_n will be incalculable. The F_n orientation determined by this technique will be the F_n orientation without the simple shear component but with the pure shear component. If the original F_n orientation could be determined by looking at an area which had undergone insignificant D_{n+1} deformation (Ramsay 1967) and the orientation of the principal axes of the pure shear component were known, it would then be possible to estimate the amount of pure shear (or volume loss) present. Weijermars (1985) has addressed the added complications to be expected if one or other, or both phases developed by dome folding (by the mechanisms proposed by Gauss 1973 and Cobbold & Quinquis 1980). Only the simplest case is considered here.

The F_n event folds S_{n-1} so that S_{n-1} is consequently of variable orientation whilst the F_n fold axes comprise a fairly linear feature across the area under analysis. When S_{n-1} surfaces are folded by F_{n+1}, the F_{n+1} fold axes developed thereon lie in and define the F_{n+1} shear plane (Carey 1962, Thiessen & Haviland 1986) (see Fig. 1). The F_{n+1} shear plane is equivalent to the second or F_{n+1} hinge plane of Thiessen & Haviland (1986). Due to F_{n+1} folding the F_n fold axes will define a plane (the F_n hinge plane) which contains the a_{n+1}-direction, i.e. the *a*-direction of the F_{n+1} fold phase. Hence by plotting fold axial data on a stereonet one can work out the shear plane and absolute movement direction of the simple shear component of the later fold phase as is illustrated in Fig. 2. This is true whether or not a component of pure shear is associated with F_{n+1}. The a_{n+1}-direction is parallel to the intersection of the two girdles defined by the two fold axial distributions. The b_{n+1}-direction will be perpendicular to the a_{n+1}-direction within the F_{n+1}

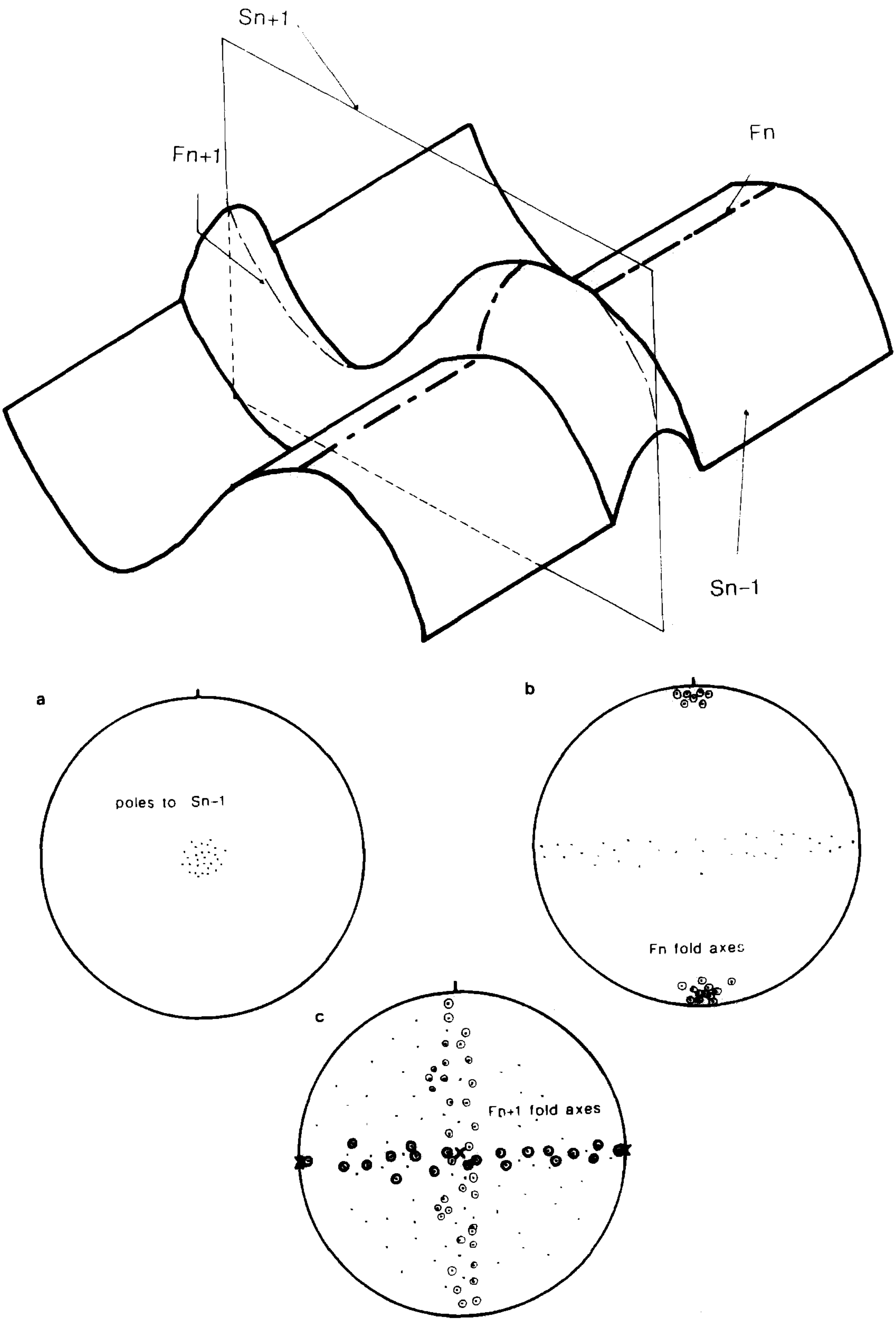

Fig. 1. An originally horizontal S_{n-1} (stereonet a; dots) is folded by F_n folds (stereonet b; lightly circled dots). F_n folds have horizontal N–S fold axes and vertical axial planes. At this stage poles to S_{n-1} have a girdle distribution. Subsequently this arrangement is refolded by F_{n+1} folds (stereonet c; heavily circled dots). Poles to S_{n-1} have a variable distribution, however the fold axes of both phases describe girdle distributions. These intersect at the a_{n+1}-direction and the b_{n+1}-direction is perpendicular to this orientation within the F_{n+1} girdle. For this case the a_{n+1}-direction is vertical and the b_{n+1}-direction is 0 to 090.

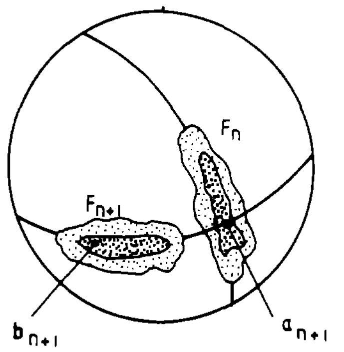

Fig. 2. The girdles described by the fold axial distributions are plotted (i.e. the hinge planes) and the intersection of these gives the a_{n+1}-direction, with the b_{n+1}-direction lying perpendicular to this within the F_{n+1} girdle.

hinge plane. This b_{n+1}-direction will be parallel to the true F_{n+1} fold axial direction (i.e. with respect to the initial S_{n-1} orientation) if, and only if, b_{n+1} lies within the initial S_{n-1} orientation. This cannot be assumed. However, b_{n+1} may be used to obtain more detailed information as to the nature of F_n (see Fig. 3).

The technique for estimating the orientational relationships of two consecutive fold phases is as follows.

(i) The data are plotted and the a_{n+1}- and b_{n+1}-directions are calculated as described above (see Fig. 2).

(ii) Two points with extreme values on the F_n fold axial distribution (P_1, P_2 in Fig. 3a) are marked. These points should be located within a fairly high contour interval or may be centres of two modes of a bimodal distribution.

(iii) With shear sense equal to that which formed the respective limbs, the angles from the a_{n+1}-direction to P_1 and P_2, are measured (see Fig. 3b). These angles are defined as x_1 and x_2, respectively. They may be measured directly from the stereonet. Equal amounts of simple shearing (equivalent in all respects, except sense, to that which formed the folds) are applied to both limbs until P_1 and P_2 lie along the one linear direction. This is an estimation of the original orientation of the F_n fold axis with respect to the F_{n+1} phase (Fig. 3a). Mathematically the value of x_1 after unfolding (which is x_1') is given by

$$\tan x_1' = 2(\cot x_1 - \cot x_2)^{-1}.$$

This method assumes fold symmetry in that the folds developed by equal amounts of simple shear on opposing limbs. Such an assumption will be largely valid for folds produced during a coaxial strain history but asymmetry is to be expected under non-coaxial deformation.

(iv) To estimate the pre-F_{n+1} orientation of S_n, the S_n axial planes corresponding to P_1 and P_2 are plotted. On Fig. 3(c) these planes are labelled S_{n1} and S_{n2}. The intersections of these planes with the F_{n+1} hinge plane gives two orientations m and n, which should, in theory, be one point. The planes containing m or n and the calculated pre-F_{n+1} F_n orientation are estimates of the pre-F_{n+1} S_n orientation (Fig. 3c, cf. Skjernaa 1980).

Because the true relationships of the fold phases are known, it is possible to apply fold interference classifications such as that proposed by Thiessen & Means (1980).

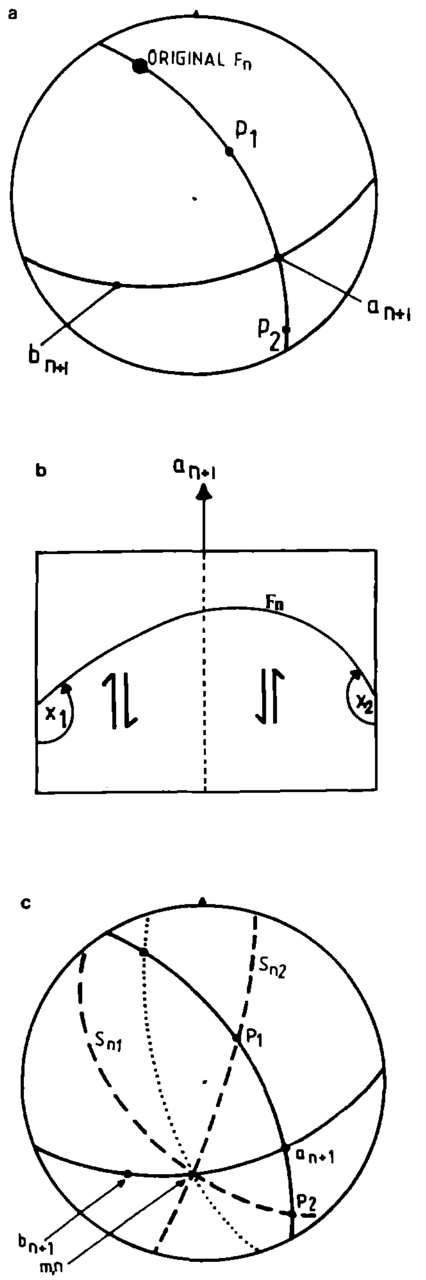

Fig. 3. (a) The a_{n+1}-direction and b_{n+1}-direction is determined for the given situation using the method illustrated in Fig. 2. The orientations of the F_n axes (P_1 and P_2), that have extreme orientations within the F_n distribution, are plotted. The angles x_1 and x_2 are measured. x_1 is the angle from a_{n+1} to P_1 measured in the same sense as the folding, x_2 is defined similarly with respect to P_2. Using the formula presented in the text, the original (pre-F_{n+1}) F_n orientation is determined and plotted. (b) The relationship between x_1, x_2 and a_{n+1}. The shear senses are those used in unshearing both limbs to determine an estimation of the original orientation of the F_n fold axis. (c) The axial planes corresponding to P_1 and P_2 (i.e. S_{n1} and S_{n2}) are plotted. These intersect the F_n girdle at m and n (theoretically the same point). The plane containing m and/or n and the original F_n orientation is an estimate of S_n (the dotted plane in the figure).

VARIABILITY IN FOLD AXIAL ORIENTATIONS

Variability in orientation of fold axes will not occur where the phases had a co-axial and/or co-planar initial spatial relationship, i.e. type 0 or type 3 interference (Ramsay 1967, Thiessen & Means 1980, Ramsay & Huber 1987). A quick glance at the data will therefore allow omission of these interference types. For data with variable orientations of fold axes, application of the reconstruction technique illustrated in Fig. 3 will enable the true nature of the relationship to be seen.

Finally, it is noted that the amount of variability in the orientation of fold axes can be attributed to four factors:

(i) the tightness of F_n; i.e. its tightness prior to F_{n+1};

(ii) the tightness of F_{n+1};

(iii) the angle between the original fold axial and axial planar directions of the respective fold phases (see Fig. 4a);

(iv) the style of folding.

In general, attainment of greater tightness by one fold phase leads to greater variability in the orientation of the fold axes of the other fold phase. Low variability is to be expected for high interlimb angles. Largest variability occurs for interlimb angles close to 90° but as interlimb angles approach zero, variability is reduced. Figure 4(b) illustrates the relationship between the third factor and variability. The angles n_1, n_2 and n_3 are defined in Fig. 4(a) and vary from 0 to 90°; note that n_3 is equivalent to the angle δ of Thiessen & Means (1980). For n_1, n_2 and/or $n_3 = 0$, the variability in both phases will be negligible. By holding one variable constant and letting the other two vary (i.e. looking at cross-sections), the relationship shown in Fig. 4(b) can be deduced; for example, the plane perpendicular to n_1, for which $n_1 = 90°$ gives the relations shown in Table 1. The curves shown in Fig. 4(b) are schematic and do not represent mathematical functions. Weijermars (1985) has already addressed the relationship between fold style and variability. Greater variability is to be expected from more rounded concentric folds as opposed to chevron styles.

Not only do the first three factors affect variability, but they also control the distribution of fold axes observed. Table 2 indicates the predicted type of distribution for each consecutive fold phase, as a function of tightness, interference pattern and style (cf. Weijermars 1985). As such, by looking at distributions from regions that have type 1 or 2 interference patterns it is possible in some cases to ascertain the tightness of F_n prior to F_{n+1}

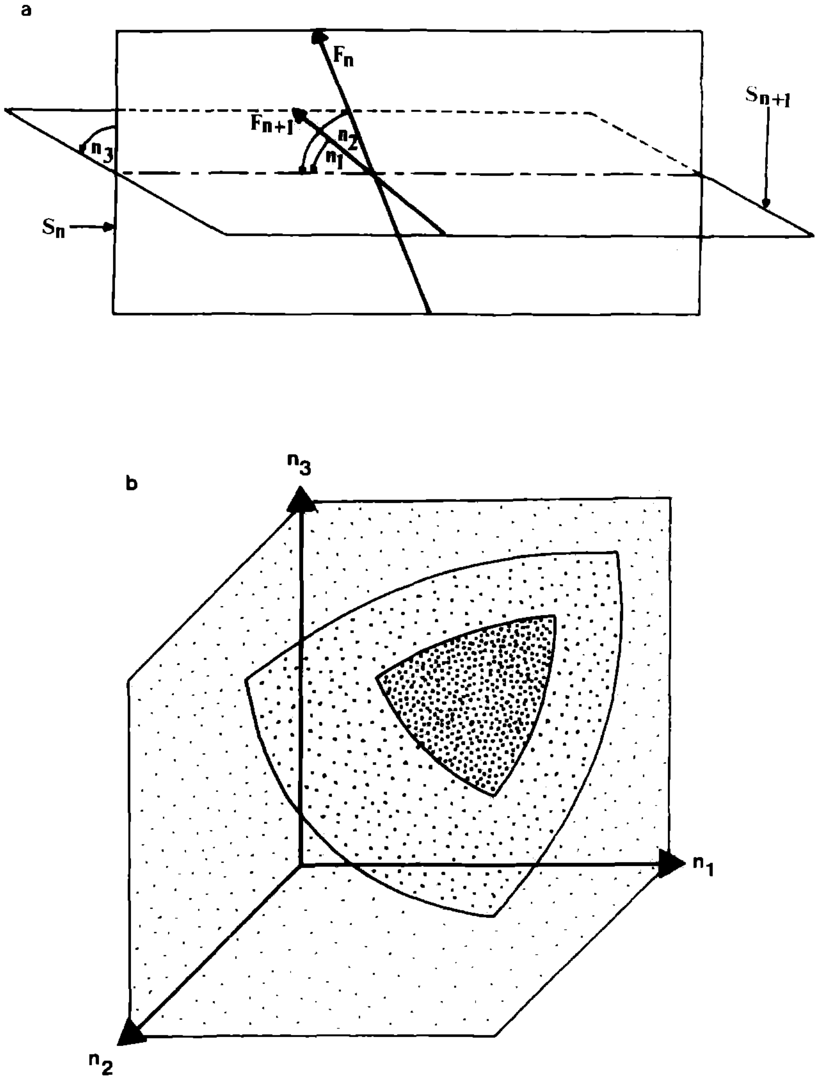

Fig. 4. (a) A definition of n_1, n_2 and n_3. n_1 is the angle between the F_n fold axis and the intersection of S_n and S_{n+1}. n_2 is the same except with respect to F_{n+1}. n_3 is the dihedral angle between S_n and S_{n+1}. (b) A schematic relationship between n_1, n_2 and n_3, and fold axial variability. The level of variability increases with the intensity of the shading pattern—light stipple (least varied), medium stipple to heavy stipple (most varied).

Table 1. With $n_1 = 90°$, n_2 and n_3 are let vary from low to high values. The corresponding variability of fold axes is tabulated as a function of these

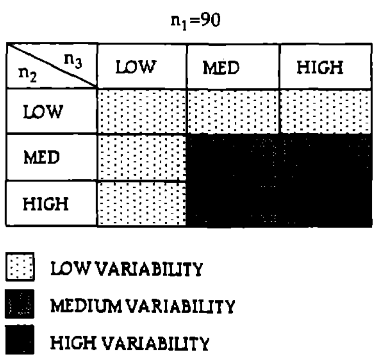

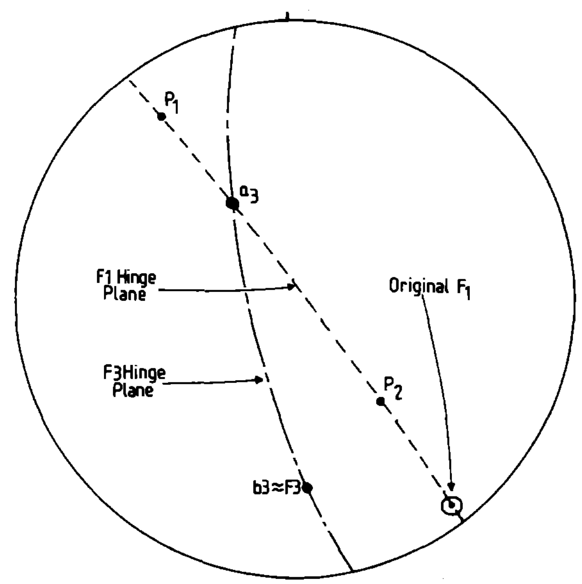

Fig. 5. Interpretation of the data from the Tabberabbera district (data from Fergusson & Gray 1989).

(i.e. whether it was isoclinal or non-isoclinal). For example, Weijermars (1985) describes early folds with a small, girdle distribution and later folds with a bimodal distribution. This was interpreted as chevron early folds non-coaxially refolded (interference type 1 or 2) by later cylindrical folds; a conclusion compatible with Table 2. The early folds were non-isoclinal, prior to F_{n+1}.

EXAMPLE

Data from the Tabberabbera district, eastern Victoria, Australia (Fergusson & Gray 1989), are used to illustrate this technique. An early fold phase affects Ordovician quartz flysch and a later, locally intense, fold phase affects the latter and an Esmian clastic sequence. F_1 folds are 'close to tight with narrow, mainly angular hinges and long planar limbs' whereas F_3 folds are close to open with low amplitude to wavelength ratios. F_1 folds are affected by F_3 within the Mitchell Syncline. Data used here was taken by Fergusson & Gray (1989) from within this area. Both fold axial distributions describe variability (F_1: bimodal-girdle, 144 87NE; F_3: girdle, possibly bimodal, 349 76W). Figure 5 shows the intersection of the two hinge planes and the a_3 and b_3 directions. The points P_1 and P_2 are also shown. The angles x_1 and x_2 are measured clockwise and anticlockwise with respect to a_3 ($x_1 = 35°$ and $x_2 = 75°$). From this the true orientation of F_1 was calculated to be 7° towards 145°. This result is in strong agreement with Fergusson & Gray's (1989) description, where they indicate that outside the influence of F_3 folding, F_1 folds are 'shallowly plunging E–W to NW–SE' folds.

DISCUSSION

The technique presented here allows easy interpretation of fold axial data and gives a three-dimensional view of the structure of a given area. Ragan (1985) and Ramsay & Huber (1987) show that multiply folded regions may be interpreted by selective plotting of bedding; however, this will only give the final orientational relationship between consecutive fold phases. By contrast, the method developed here strives to delimit the original orientational relationships of the respective fold phases. Caution must be taken to ensure that the technique is applied within a tectonically homogeneous domain.

It must be reiterated that the technique is simplistic in that it assumes that equal amounts of shear strain developed on opposing F_{n+1} limbs. This may not be the case particularly in regions having undergone a simple shear D_{n+1} strain history. It must also be noted that perfect shear folds are rarely encountered in nature; many folds approximate to this morphogenetic category. Also, the effect of early fold shapes on interference patterns was not considered in this study (Ghosh & Ramberg 1968, Skjernaa 1975, Watkinson 1981). However, Thiessen & Haviland (1986) have demonstrated that this factor is not important. This results from the stipulation that the second fold phase must develop by shear folding. De-

Table 2. The relationship between tightness/style of the respective fold phases, interference type and the resulting distribution of the fold axes of both phases. Tightness of F_n refers to the tightness prior to F_{n+1}. The non-isoclinal categories are: Con = concentric and Chv = chevron. The distribution types are U = unimodal, B = bimodal and G = girdle

Tightness and style	Iso	Iso	Iso	Con	Chv	Chv	Con	Chv	Con	Any	F_{n+1}
	Iso	Con	Chv	Iso	Iso	Chv	Chv	Con	Con	Any	F_n
Distribution	U	G	B	U	U	B	B	G	G	U	F_{n+1}
	B	B	B	G	B	B	G	B	G	U	F_n
Inference type					1 or 2					0 or 3	

spite the above criticisms the model presented here serves as a first approximation in many cases.

Weijermars (1985) states that the interpretation of fold axial distributions of early (F_n) folds is problematical, particularly if the assumption of cylindricity of either of the fold phases is removed. Table 1 of Weijermars (1985) describes the interpretation of distributions with and without the assumption of cylindricity, whereas Table 2 of this paper only addresses the case of cylindricity.

The technique presented in this paper is similar to that of Thiessen & Haviland (1986) in so far as they showed how the original orientation of the earlier fold phase could be estimated. However, the present technique has some advantages. Thiessen & Haviland (*op. cit.*) describe Ramsay's method of multiple a_{n+1} orientations; this is not a requirement of the present technique. Further, data can be analysed in bulk, rather than in portions, when using the present method. To determine S_n Thiessen and Haviland's method requires that several sections through the deformed rock mass are available, such that traces of the first axial plane of one particular fold are traceable. Normally this would only be available from small samples. The technique presented here is applicable on all scales.

CONCLUSIONS

(i) A technique for the interpretation of fold axial data in regions with two fold phases, allowing the determination of the original orientations of the respective fold phases, has been presented.

(ii) Two interfering fold phases, in general, produce a variability in fold axial orientations unless the interference pattern is of type 0 or 3.

(iii) Variability is largely proportional to tightness, style and the relative orientations of the respective fold phases.

(iv) Under the assumption of cylindricity, fold axial distributions can give information regarding the pre-F_{n+1} style and tightness (i.e. chevron or concentric; isoclinal or non-isoclinal) of F_n.

Acknowledgements—Thanks to Mr E. Edwards, Dr A. R. Allen, Mr P. Meere and Dr C. Mitchell for reading and criticizing earlier drafts of this manuscript. The paper benefited greatly from the comments of the two anonymous reviewers. This paper was presented in poster form at T.S.G. 1988, travel expenses were provided by the Geology Department, U.C. Cork.

REFERENCES

Carey, S. W. 1962. Folding. *J. Alberta Soc. Petrol. Geol.* **10**, 95–145.
Cobbold, P. R. & Quinquis, H. 1980. Development of sheath folds in shear regimes. *J. Struct. Geol.* **2**, 119–126.
Fergusson, C. L. & Gray, D. R. 1989. Folding of angular unconformable sequences and effects on early folds, Tabberabbera district, eastern Victoria, Australia. *Tectonophysics* **158**, 93–111.
Gauss, G. A. 1973. The structure of the Padstow area, North Cornwall. *Proc. Geol. Ass.* **84**, 283–313.
Ghosh, S. K. & Ramberg, H. 1968. Buckling experiments on intersecting fold patterns. *Tectonophysics* **5**, 89–105.
Hobbs, B. E., Means, W. D. & Williams, P. F. 1976. *An Outline of Structural Geology*. Wiley International, New York.
Ragan, D. M. 1985. *Structural Geology, An Introduction to Geometrical Techniques* (3rd edn). John Wiley, New York.
Ramsay, J. G. 1967. *The Folding and Fracturing of Rocks*. McGraw-Hill, New York.
Ramsay, J. G. & Huber, M. I. 1987. *The Techniques of Modern Structural Geology, Volume 2: Folds and Fractures*. Academic Press, London.
Skjernaa, L. 1975. Experiments on superimposed buckle folding. *Tectonophysics* **27**, 255–270.
Skjernaa, L. 1980. Rotation and deformation of randomly oriented planar and linear structures in progressive simple shear. *J. Struct. Geol.* **2**, 101–109.
Thiessen, R. L. & Means, W. D. 1980. Classification of fold interference patterns: a re-examination. *J. Struct. Geol.* **2**, 311–326.
Thiessen, R. L. & Haviland, T. 1986. A technique for the analysis of refold structures. *J. Struct. Geol.* **8**, 191–200.
Watkinson, A. J. 1981. Patterns of fold interference: influence of early fold shapes. *J. Struct. Geol.* **3**, 19–23.
Weijermars, R. 1985. Directional variations of fold axes in progressive deformation, an example from a Betic fold nappe in S. Spain. *Geologie Mijnb.* **64**, 271–280.